Int. J. Electrochem. Sci., 7 **(2012)** 3610 - 3626

International Journal of
ELECTROCHEMICAL
SCIENCE
www.electrochemsci.org

Synthesis and Photoelectrochemical Behavior of a Hybrid Electrode Composed of Polyaniline Encapsulated in Highly Ordered TiO_2 Nanotubes Array

Nada F, Atta[*]*, Ahmed Galal, Hatem M. A. Amin*

Department of Chemistry, Faculty of Science, Cairo University, Postal Code 12613, Giza, Egypt
[*]E-mail: nada_fah1@yahoo.com

Received: 19 January 2012 / *Accepted:* 2 March 2012 / *Published:* 1 April 2012

Polyaniline (PANI) nanostructures encapsulated in highly ordered TiO_2 nanotubes (NT_s) array was obtained by formation of TiO_2 NT_s array in HF-H_3PO_4 solution using constant potential anodization method; followed by electropolymerization of aniline to be encapsulated in the TiO_2 NT_s array, The electrochemical , morphological and structural characteristics of PANI/TiO_2 nanocomposite electrode were examined by cyclic voltammetry (CV), electrochemical impedance spectroscopy (EIS), scanning electron microscope (SEM), X-ray diffraction (XRD) and infrared (IR) spectroscopy. Thermal behavior of PANI film was studied by thermogravimetric analysis (TGA). Studies showed that anatase phase of TiO_2 prevailed and PANI-modified TiO_2 composite did not change the crystalline structure of neat TiO_2. Dye sensitized photogalvanic cell based on PANI/TiO_2 nanocomposite electrode was also examined. Different metal phthalocyanine dyes were examined as the photosensitizer for composites formed of PANI nanostructures encapsulated in TiO_2 NT_s array. The Photoelectrochemical properties and the conversion efficiency of the modified CoPC dye sensitized PANI/TiO_2 nanocomposite were enhanced compared to "neat" TiO_2 NT_s. The photogalvanic cell showed good stability for many turnovers.

Keywords: TiO_2 nanotubes; Dye sensitized solar cell; Polyaniline; Phthalocyanine; Photoelectrochemical properties.

1. INTRODUCTION

Dye sensitized solar cells ($DSSC_s$) based on nanocrystalline TiO_2 have attracted much attention since their first description at the beginning of the 1990_s by O'Reagan and Grätzel [1]. $DSSC_s$ are currently attracting extensive academic and industrial interest envisioning this technology as a powerful and promising way to generate electricity from the sun at low cost with high efficiency. TiO_2 is a widely used semiconductor due to its high stability, favorable bandgap energy, abundant

availability, and inexpensive cost [2]. As compared with randomly distributed titania nanowires, the well-aligned titania nanotubes arrays, especially the single crystalline one, enhanced the charge collection and transport rate and in turn the light conversion efficiency [3]. Titania nanotube arrays deposited either on transparent conducting oxide coated glass substrates [4] or metallic Ti substrates [5] are also believed to be ideal candidates of photoanodes for high-efficiency $DSSC_s$. The electron produced at the surface of nanotube can be directly transported into a current collector without large point contact resistance which occurred at the boundary between nanoparticles.

$DSSC_s$ have gained much attention in recent years because of their potential low cost, low environmental impact, and power conversion efficiency comparable to conventional solar cells [6]. Nowadays, high efficiencies have been reported for DSSC using liquid electrolytes and a ruthenium complex as sensitizer [7]. Several research groups have considered novel dyes, since the loss in efficiency after a long period of solar exposition is attributed to the ruthenium complex (the most common are the N3 and N719 dyes) unstability [8]. The main drawbacks of these sensitizers are the lack of absorption in the red region of the visible spectrum and also relatively low molar extinction coefficient above 600 nm. In addition, the high cost of the ruthenium complexes and the potential unavailability of this noble metal have triggered the search for less expensive and stable sensitizers. In contrast, phthalocyanines possess intense absorption bands in the near-IR region and are known for their excellent chemical, photo and thermal stability; and have appropriate redox properties for sensitization of wide bandgap semiconductors, e.g., TiO_2, rendering them attractive for DSSC applications [9].

Although $DSSC_s$ can show high conversion efficiency, there are remaining some significant limitations, in particular the liquid redox electrolyte which leads to several technical disadvantages [10]. Thus, there are practical benefits for replacing the liquid electrolyte system with solid conductive materials. Conducting polymers are promising candidates that could be used as charge transport materials. They have attracted much attention among both researchers and society since their discovery. This has been driven by the exceptional electronic, optical and magnetic properties of these materials that provide a vast range of potential applications [11, 12]. Polyaniline (PANI) is the most extensively investigated conducting polymer because of its unique reversible protonic dopability, excellent redox reversibility, environmental stability, variable electrical conductivity, low cost and easy synthesis [13]. The ability of PANI to exist in various forms via acid/base treatment and oxidation /reduction, either chemically or electrochemically, has made PANI the most tunable member of the conducting polymer. K. Lim and co-workers [14] synthesized conducting PANI – titanium dioxide (TiO_2) composite micron-sized rods using an in situ gamma radiation-induced chemical polymerization method. Polypyrrole encapsulated in highly ordered TiO_2 nanotubes array electrode was prepared by L. Jin et al. [15]. Murakoshi et al. [16] reported a cell with photopolymerized pyrrole on porous nanocrystalline TiO_2 in which the polypyrrole acted as a hole transport layer. It showed an improvement of the cell characteristics when polypyrrole was covalently bonded to the dye. The overall efficiency was improved to 0.1% after $LiClO_4$ was used to dope the resulting polypyrrole. PANI has been used as electrode material based on its reversible electrochemical redox reaction. In particular for TiO_2 photoelectrode catalytic process in presence of PANI, TiO_2 photoelectrode can be excited with irradiation and the photogenerated electrons can be captured by PANI and quickly

transferred to counter electrode. Thus, by incorporating PANI nanoparticles in TiO_2 NT_s photoelectrode, the enhanced photoelectrochemical performance is expected. The effect of changing illumination intensity on the conversion efficiency and short circuit current (Jsc) was previously studied [17].

In this paper, the highly ordered TiO_2 NT_s array prepared by constant potential anodization method in HF-H_3PO_4 solution acted as a reactive photoelectrode material. PANI was used as a chemical modifying reagent, as well as efficient electrons trapper. PANI/TiO_2 nanocomposite electrode was prepared by electropolymerization of aniline forming PANI nanostructures inside/over TiO_2 NT_s in order to enhance the photoelectrochemical conversion efficiency. Characterization of PANI/TiO_2 nanocomposite electrode under different conditions was also reported. The applicability of PANI/TiO_2 nanocomposite electrode to photoelectrochemical energy conversion using different metal phthalocyanine dyes was studied in dark and under illumination. The incorporation of conducting PANI nanostructures into TiO_2 NT_s was found to enhance the photoelectrochemical response of the composite. Cobalt phthalocyanine (CoPC) dye showed the best conversion efficiency compared to the other studied phthalocyanine dyes.

2. EXPERIMENTAL

2.1. Preparation of a hybrid PANI/TiO_2 nanocomposite electrode

Polyaniline encapsulated in highly ordered TiO_2 nanotubes array (PANI/TiO_2 NT_s) electrode was obtained via two steps: (1) electrosynthesis of TiO_2 nanotubes array electrode by constant potential anodization process as shown in our previous work [18]. Prior to anodization, the Ti rod electrode was first mechanically polished with different abrasive papers and Alumina (2 μm) /water slurry on BUEHLER pads and cleaned in ethanol (for 10 min.) and then in acetone (for 10 min.) and then chemically polished in strong acidic solution of HF (3.3 mol L^{-1})-HNO_3 (5.6 mol L^{-1}) for 15 seconds to form a fresh smooth surface. Ti electrode was then rinsed with water and dried in air at room temperature. The TiO_2 NT_s electrode was fabricated in a cylindrical Teflon cell equipped with a regulated direct current (DC) power supply with a two-electrode configuration, in which the pre-treated Ti electrode was used as the working electrode for an anode role and a platinum sheet acting as the counter electrode. Anodization process was carried out at 20 V in 0.15 mol L^{-1} HF + 0.5 mol L^{-1} H_3PO_4 electrolyte for 40 minutes.

After anodization, the electrode was thoroughly rinsed with distilled water and subsequently in acetone, and finally dried in air. Anodized Ti electrode was annealed in an oven at 105 ˚C for 12 hours. Finally, the electrode was calcinated at 450 ˚C for 2 hours. A well-ordered TiO_2 NT_s array was obtained under the aforementioned "optimized" conditions. (2) The electropolymerization of aniline was carried out in a three-electrode/one-compartment glass cell in the 1 mol L^{-1} H_2SO_4 solution containing 0.3 mol L^{-1} aniline monomer (aniline was distilled prior to use). The fabricated TiO_2 NT_s electrode was used as the working electrode, a saturated Ag/AgCl electrode and a platinum sheet served as reference and counter electrode, respectively. The PANI film was electropolymerized with a

Cyclic Voltammetry (CV) method at the potential range from -0.1 V to 1.2 V with 100 mV s^{-1} scan rate.

A second method was used to form PANI films ca. by applying a constant potential at the fabricated TiO_2 NTs (bulk electrolysis, BE). The color of PANI film formed was green. The electrode was rinsed carefully with distilled water then PANI/TiO_2 nanocomposite electrode was obtained.

2.2. Characterization of PANI/TiO_2 nanocomposite electrode

Scanning electron microscope (SEM) with Philips XL 30 instrument was used to investigate the morphology of TiO_2 NT_s array and modified PANI/TiO_2 nanocomposite. Samples investigated by SEM were prepared as previously mentioned in the experimental section (2.1). The SEM images were processed with a personal computer connected to the SEM. The crystalline structure and the phase purity of TiO_2 and PANI modified TiO_2 samples were analyzed by X-ray diffraction (PANalytical X'pert PRo XRD instrument) with Cu K_α radiation operating at 45 kV and 40 mA. XRD patterns of TiO_2 and modified PANI/TiO_2 films were collected at a scan rate of 4º /min in the 2θ range of 20º – 80º. The thermal properties and stability of PANI were investigated using thermal gravimetric analysis (TGA). TGA was performed using a Schimadzu DTG-60H instrument. Heating rate was 10˚C/minute and inert gas used was purified nitrogen.

The formation of the polymer film was ascertained by using IR spectroscopic technique. IR transmission measurements were carried out by mixing samples with spectra-grade KBr. The IR transmission spectra were obtained on a Brucker Vector 22, Germany. Sixty four scans were performed at a resolution of 2 cm^{-1} and with accuracy of 0.004 cm^{-1} between 4000 and 400 cm^{-1}. Electrochemical polymerization and characterization experiments of PANI by CV were carried out using a BAS-100B (BAS Inc., USA) at room temperature (25 °C ± 2 °C) in the monomer free solution (1 mol L^{-1} H_2SO_4) between the two following potential limits: E_i= -0.1 V and E_f = 1.2 V, scan rate = 50 mV s^{-1}.

Electrochemical impedance spectroscopy (EIS) has been widely employed to study the kinetics of electrochemical and photoelectrochemical processes occurring in the dye sensitized solar cells. In this study, impedance spectrum analysis had been applied to explore the electric conductivity of the composite electrode [1] under open-circuit potential (OCP) over the frequency range of 0.1 Hz-100 kHz and ac-voltage amplitude of 10 mV. One of the factors affecting the photoelectrochemical and chemical processes studied by EIS was the effect of illumination.

The EIS measurements for the PANI/TiO_2 electrode prepared under optimized conditions were performed at room temperature in 10^{-3} mol L^{-1} dye/1 mol L^{-1} H_2SO_4 solution in dark and under illumination. The EIS measurements were carried out with Gamry-750 system and a lock-in-amplifier that are connected to a personal computer.

The data analysis software was provided with the instrument and applied non-linear least square fitting with Levenberg-Marquadt algorithm. The best fitting values calculated from the equivalent circuit for the impedance data were reported.

2.3. Photoelectrochemical measurements

I-V characteristics of the electrodes prepared at different conditions were recorded in a dye electrolyte at room temperature using Gamry-750 system in dark and under illumination of 100 mW cm^{-2}. The conversion efficiency (η) and the fill factor (FF) of the prepared solar cell systems were calculated from I-V parameters.

3. RESULTS AND DISCUSSION

3.1. Characterization of PANI/TiO_2 nanocomposite electrode

3.1.1. Cyclic voltammetry (CV)

Figure 1 shows the repeated cyclic voltammograms (CV_s) for 15 cycles during the electropolymerization of ANI. The electrolyte solution contains 0.3 mol L^{-1} ANI monomer in 1 mol L^{-1} H_2SO_4 aqueous solution.

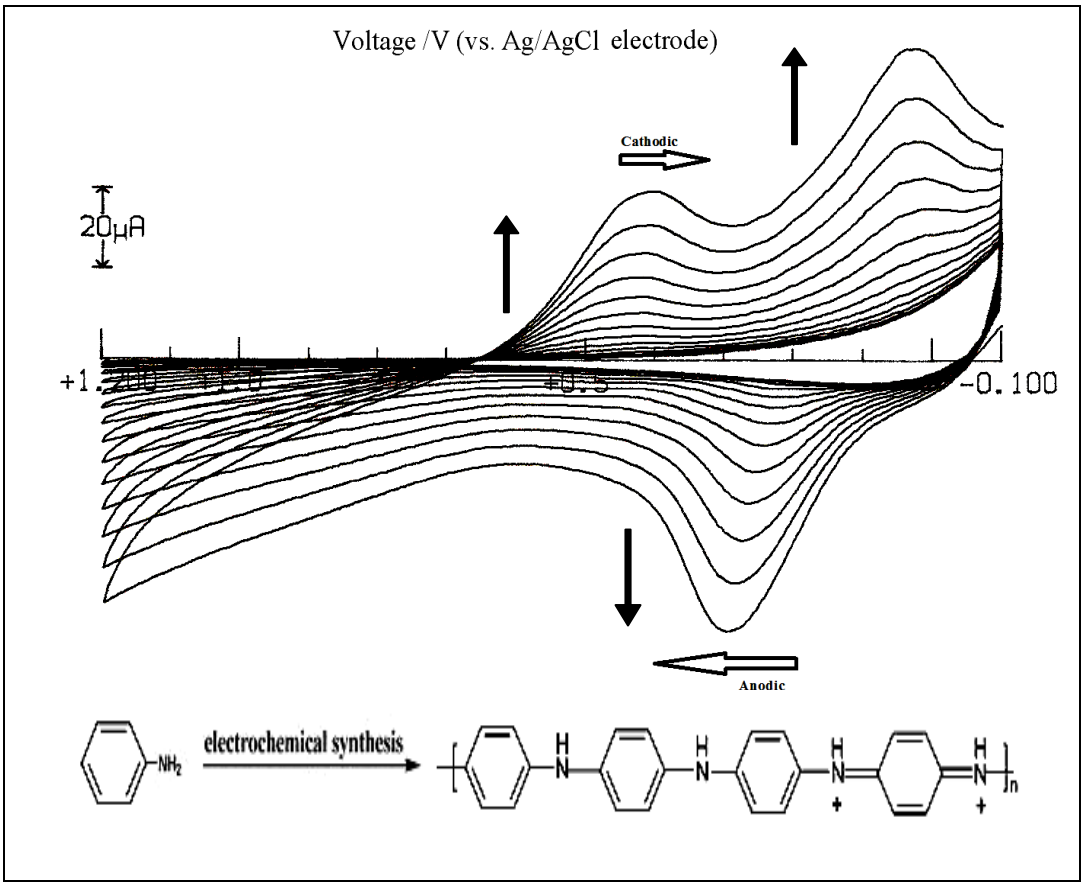

Figure 1. Repeated CVs for the formation of PANI on TiO_2 NT_s. Monomer solution: 0.3 mol L^{-1} ANI in 1 mol L^{-1} H_2SO_4 solution, scan rate = 100 mV s^{-1}, E_i = -0.1V, E_f = +1.2V for 15 cycles.

The working electrode was TiO_2 NT_s electrode previously prepared as mentioned in the experimental section. Ag/ AgCl and pt sheet serve as the reference and counter electrodes, respectively.

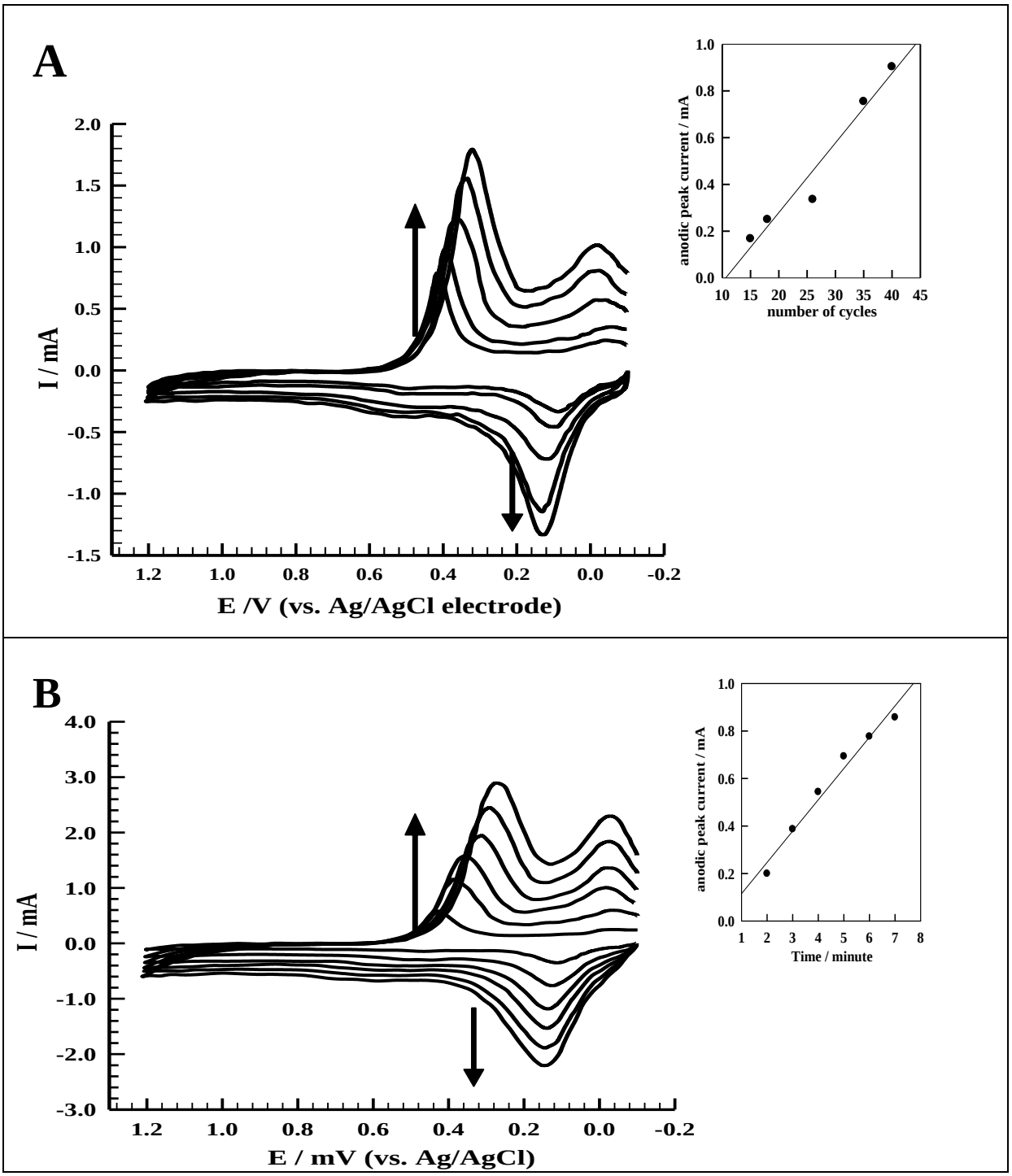

Figure 2. CV_s obtained at PANI formed by: (A) repeated cycles (15, 18, 26, 35 and 40 cycles, scan rate = 50 mV s^{-1}, E_i = -0.1 V, E_f = +1.2 V), (B) applying constant potential ($E_{applied}$ = +1.2 V) for different times (2, 3, 4, 5, 6, 7 minutes) in 1 mol L^{-1} H_2SO_4 aqueous solution. The inset represents the relationship between anodic peak current and the number of cycles (A) or polymerization time (B).

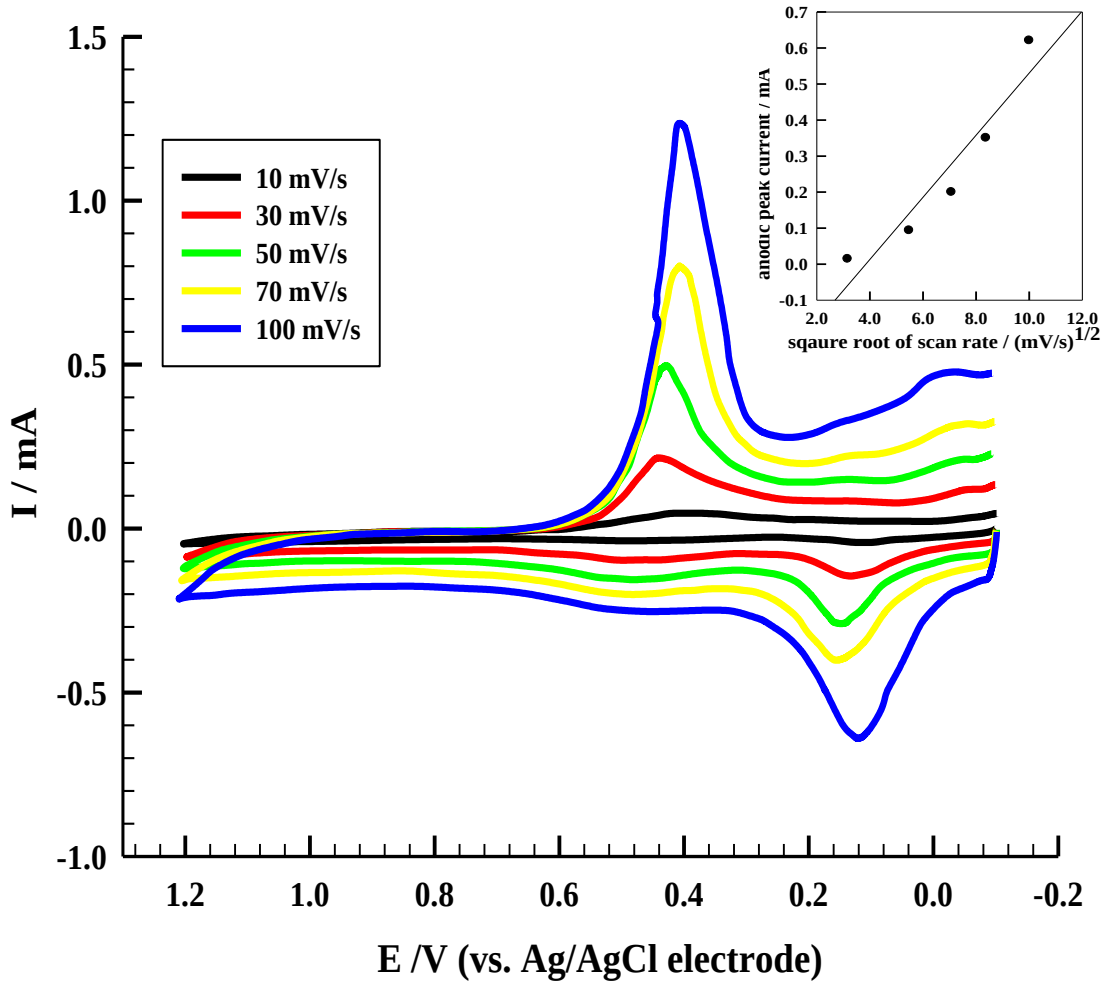

Figure 3. Cyclic voltammograms obtained in 1M H_2SO_4 aqueous solution at scan rate 10, 30, 50, 70 and 100 mV s^{-1}, E_i = -0.1V, E_f = +1.2V. The inset represents relation between anodic peak current and square root of scan rate, $\nu^{1/2}$.

The electrode potential was continuously swept between -0.1 V and +1.2 V vs. Ag/AgCl reference electrode at scan rate of 100 mV s^{-1}.

Two major redox couples are observed in these CV_s. In the positive sweep, the first redox peak (at ca. 100-300 mV) is well-known as the formation of radical cations (polaronic emeraldine); and the second redox couple at ca. 400 mV for reduction and beyond 400 mV for oxidation is due to the formation of diradical dications (represented by the resonance structures: bipolaronic pernigraniline and protonated quinonediimine) [19, 20] through the oxidation of PANI deposited on the electrode surface. The first peak current increased continually with successive potential scans, indicating that the electroactive and conductive PANI was deposited on the electrode surface [21]. The peak current rises with successive potential scan illustrating the over-oxidation and further thickening of the film.

The electrochemical behavior of PANI is expected to differ according to the method of its electropolymerization. Figure 2 shows the cyclic voltammetric response of PANI films formed with different thicknesses using repeated cyclic voltammetry (15, 18, 26, 35 and 40 cycles) Figure 2A and

constant applied potential of +1.2 V (for 2,3,4,5,6 and 7 minutes) Figure 2B, respectively, in 1 mol L^{-1} H_2SO_4 solution. The potential limits used during cycling (ca. E_i = -0.1 V and E_f = +1.2 V) indicate that the polymer film is cycled between its oxidized (doped) and reduced (undoped) states. The CV_s of Figure 2 show that the current response increases with thickness which may be attributed to the increase in the number of active sites responsible for dopant exchange. Thus, the films were conductive and also electroactive. Moreover, the amount of dopants exchanged during the oxidation-reduction process increases. This is a logical consequence of the increased capacity of the film. The sharpness of the anodic and cathodic peaks varies with thickness which indicates the distinct difference in the mechanism of charge exchange for these films.

The effect of changing scan rate on anodic peak current is shown in Figure 3 for PANI film formed by applying constant potential of +1.2V for 3 minutes. As could be noticed from the inset of Figure 3, the relation between the anodic peak current ($I_{p,a}$) and square root of scan rate ($v^{1/2}$) is linear. The observed linearity can be taken as an evidence for thin film formation and the diffusion controlled the oxidation-reduction process.

3.1.2. SEM analysis

To investigate the surface morphology of TiO_2 NT_s and modified PANI/TiO_2 electrodes, scanning electron microscopy measurements were conducted. The pore size of TiO_2 NT_s can be tuned as required by changing the synthesis parameters [18, 22, 23]. Thus, TiO_2 NT_s array was prepared under optimized conditions by applying constant potential anodization at 20 V for 40 minutes in 0.15 mol L^{-1} HF + 0.5 mol L^{-1} H_3PO_4 aqueous solution at room temperature then annealed and calcinated at 450 ˚C for 2 hours. Figure 4A shows SEM image of TiO_2 electrode, which reveals that highly ordered and quite uniform TiO_2 nanotubes array with an average pore diameter of 110 nm was fabricated by the anodization technique. Figure 4B shows the SEM image of TiO_2 NT_s electrode encapsulating PANI nanostructures which indicates the differences of the surface morphology between these two electrodes.

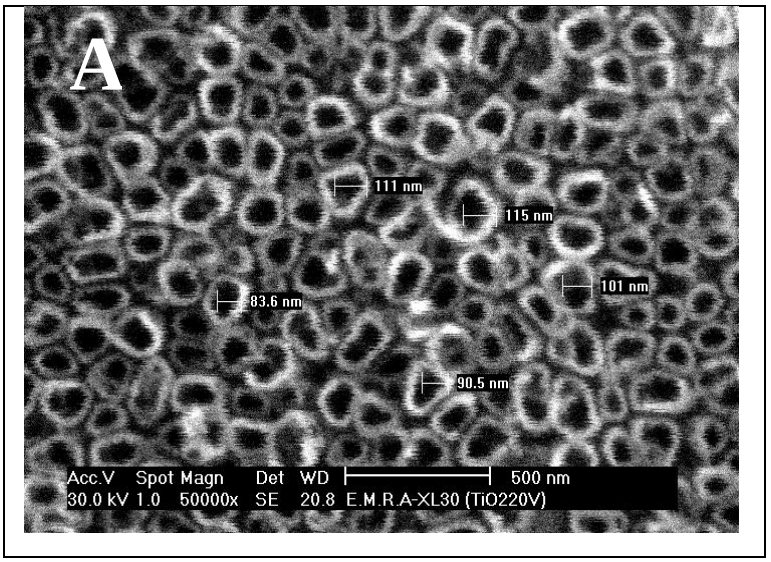

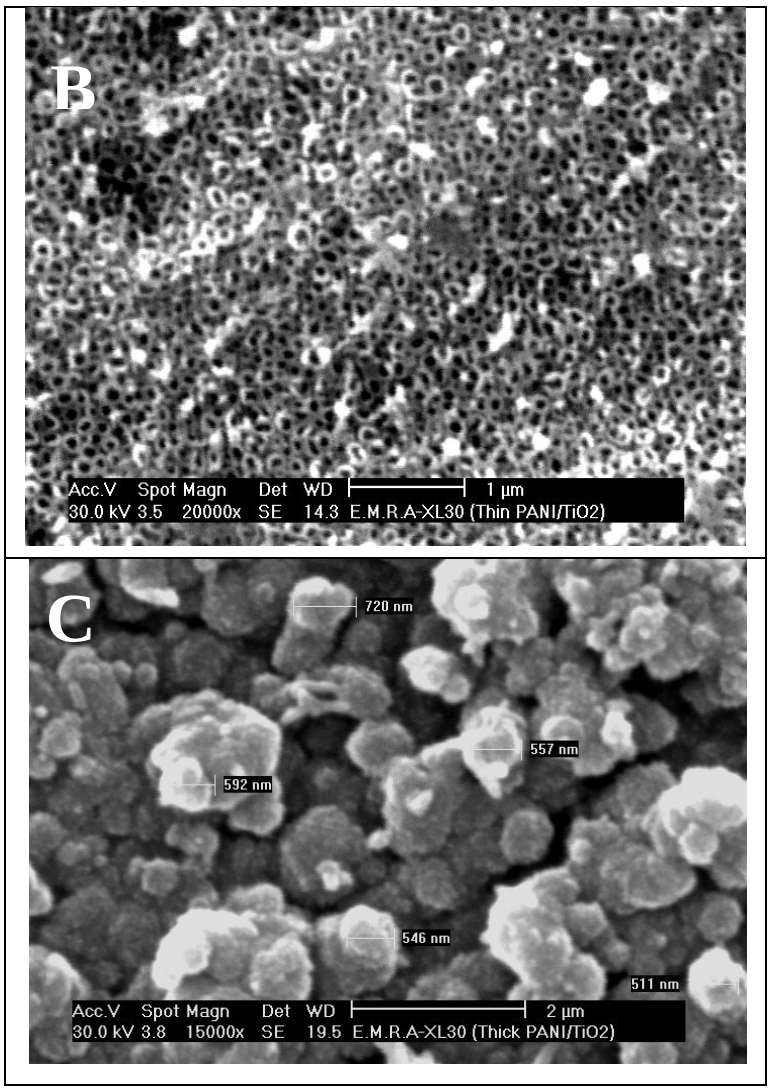

Figure 4. SEM images of TiO_2 NT_s electrode before (A) and after formation of PANI very thin film (B) or PANI thick film (C).

Aniline is electropolymerized to form PANI nanostructures inside and over the TiO_2 nanotubes. Therefore, the PANI was encapsulated on the outer-wall and the inner-wall of the TiO_2 NT_s. Figure 4C shows the SEM image of TiO_2-NTs/PANI electrode in which PANI was formed as a thick film enough to fill and cover all TiO_2 NT_s in which they did not appear from the top view of the electrode.

3.1.3. XRD analysis of TiO_2 and modified PANI/TiO_2 electrodes

To determine the crystal phases of TiO_2 NT_s and PANI/TiO_2 nanocomposite electrodes, the XRD measurements were carried out and the XRD patterns are shown in Figure 5. In the patterns, anatase TiO_2 diffraction peaks at 25.3°, 37.8° and 48.1° appeared which are attributed to the 101, 004 and 200 reflections, respectively. This indicates that only anatase phase of TiO_2 can be indexed from the patterns, and that the rutile and brookite phases of TiO_2 are not observed. Ti peaks with hexagonal

structure appear clearly-underlying matrix. Moreover, PANI modified TiO_2 composite does not cause any change in peak positions and shapes compared to neat TiO_2. This shows that PANI-modified TiO_2 composite does not change the crystalline structure of neat TiO_2. It is also noticed that no new diffraction peaks appear in the pattern of PANI-modified TiO_2 composite. This suggests that PANI is amorphous in the composite [24].

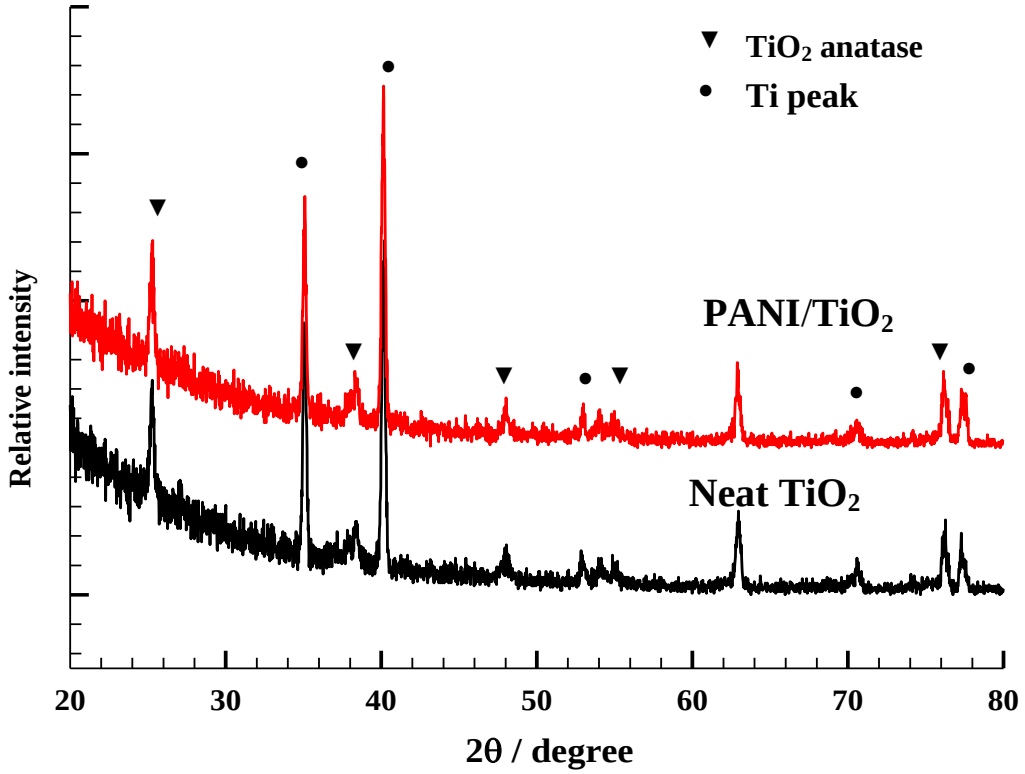

Figure 5. XRD patterns of neat TiO_2 and PANI/TiO_2 modified electrodes.

3.1.4. IR spectroscopy

The current IR investigation was aimed to ascertain the formation of the PANI film. Figure 6 shows the FT-IR spectra, in the range of (400-4000 cm^{-1}), of KBr pressed pellets of PANI. In the PANI spectrum, there is a correlation with previously reported results [24, 25]. The bands at 1490 and 1559 cm^{-1} show the characteristic C=N and C=C stretching of the quinoid and benzoid rings, respectively. The peaks at 1288 and 850 cm^{-1} can be assigned to the C-N stretching of the secondary aromatic amine and an aromatic C-H out-of-plane bending vibration on 1,4-ring, respectively. The peak at 3417 cm^{-1} can be attributed to the N-H stretching mode. The in-plane bending vibration of the C-H on 1, 4-ring is observed at about 1172 cm^{-1} which was formed during protonation. This means that the PANI formed in and over TiO_2-NTs is 1, 4-disubstituted [26].

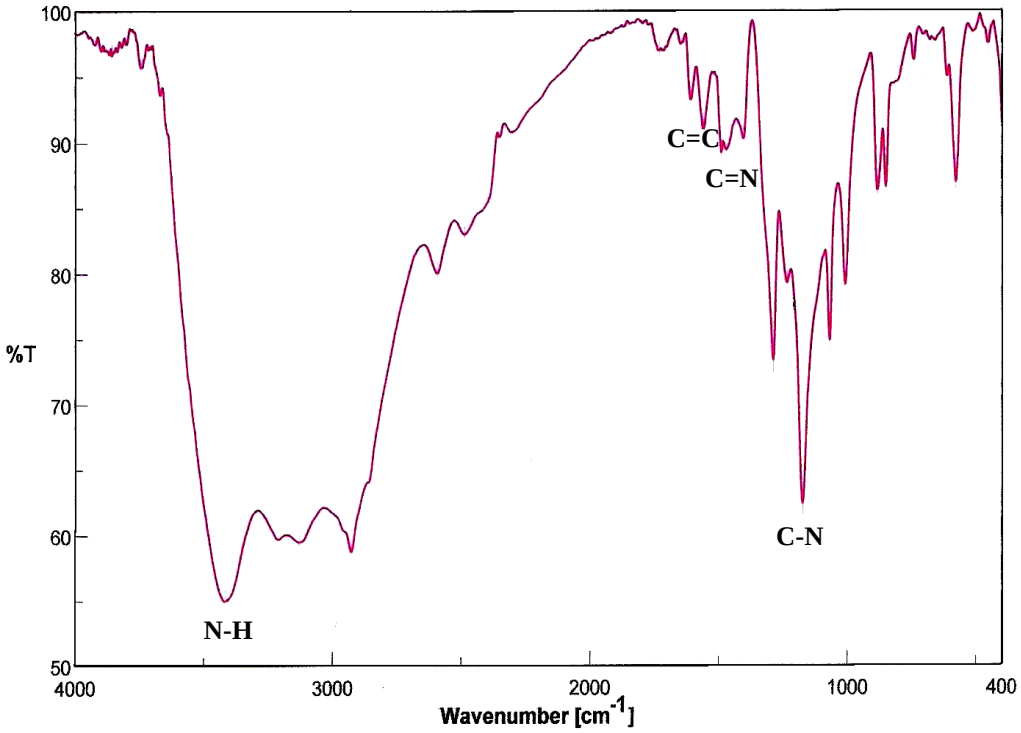

Figure 6. FT-IR spectrum for PANI prepared from 0.3 mol L^{-1} ANI in 1 mol L^{-1} H_2SO_4 aqueous solution by applying +1.2 V vs. Ag/AgCl reference electrode.

3.1.5. Thermogravimetric analysis (TGA)

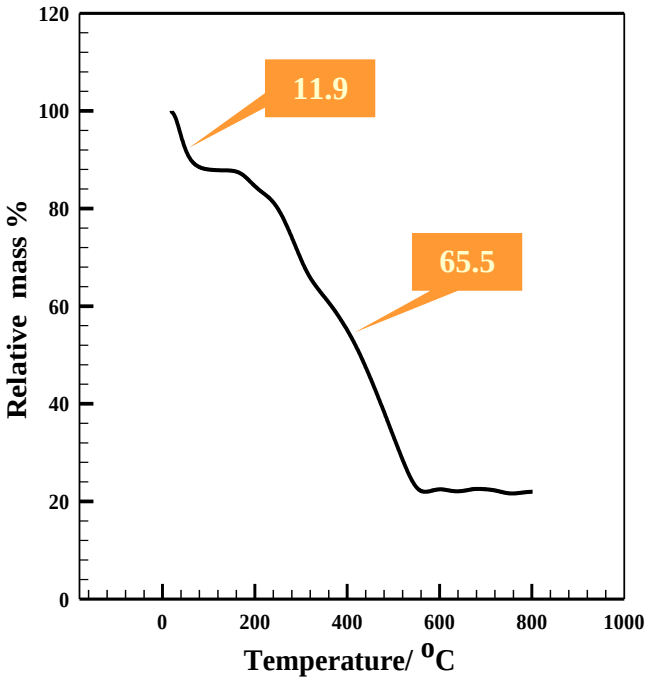

Figure 7. TGA data for PANI prepared from 0.3 mol L^{-1} ANI in 1 mol L^{-1} H_2SO_4 aqueous solution by applying +1.2 V vs. Ag/AgCl reference electrode.

3.2. Photoelectrochemical properties of the electrodes

3.2.1. Effect of PANI formation on the performance of PANI/TiO_2 electrode

The photoelectrochemical response of the PANI/TiO_2 NT_s electrode and TiO_2 NT_s electrode were investigated using I-V characteristic curve in 10^{-3} mol L^{-1} CoPC dye solution. The photovoltammetry can be used to evaluate both the electrochemical behavior with light off and the photoelectrochemical behavior with light on under the same experimental conditions [28]. The results of the photoelectrochemical response of PANI/TiO_2 NT_s electrode and TiO_2 NT_s electrode are given in Figure 8. The higher photoelectrochemical conversion efficiency of PANI/TiO_2 NT_s electrode (0.26%) compared to that of TiO_2 NT_s electrode (0.18%) under illumination of 100 mW cm^{-2} is explained in terms of the close matching of the band-gap energies of TiO_2 (3.2 eV) and PANI (2.8 eV) which enhances the charge separation and the electron transfer processes under illumination. Therefore, the photogenerated electrons on TiO_2 surface under illumination can be transferred fast through PANI film since it is a conductive film, thus the recombination of photogenerated holes and electrons can be restrained. It is concluded that the photoelectrochemical response enhanced by the formation of conducting PANI film inside/over TiO_2 NT_s.

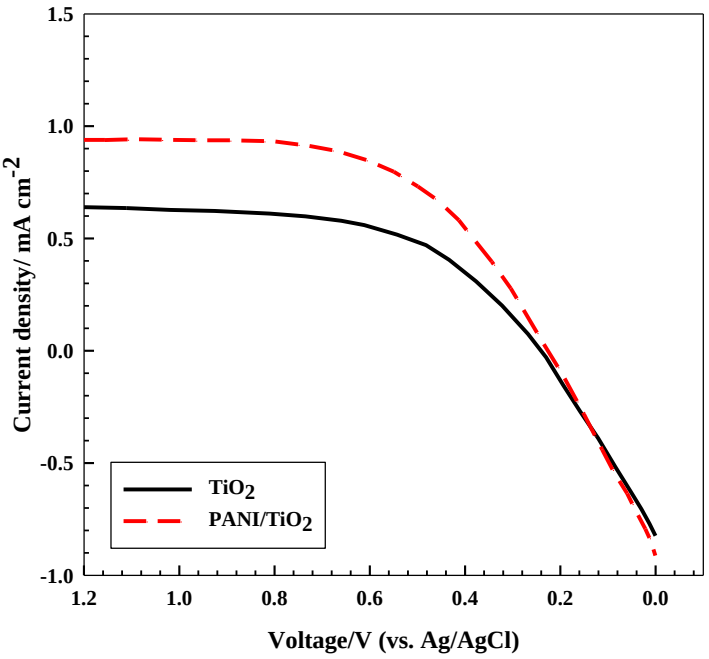

Figure 8. I-V curves of neat TiO_2 and PANI/TiO_2 electrodes tested in CoPC dye solution under illumination.

3.2.2. Effect of PANI thickness

I-V measurements were used as a guide to show the effect of changing the polymer thickness on the photoelectrochemical response of the modified PANI/TiO_2 electrode. Moreover, the results prove the synergetic effect on the photoelectrochemical process due to the PANI film. Different PANI

film thicknesses were prepared by CV by varying the number of repeated cycles for preparation of PANI over TiO_2 NT_s electrode. The prepared electrodes were tested in 10^{-3} mol L^{-1} CoPC dye solution under illumination of 100 mW cm^{-2}. I-V performance characteristics obtained from the curves are reported in table 1. By changing the thickness of PANI film over TiO_2 NT_s, the conversion efficiency of the modified electrodes changes. The conversion efficiency increases as the thickness increases up to a given thickness corresponding to films formed up to 25-30 cycles (that corresponds to a polymer film thickness 175-200 nm). This is attributed to the fact that PANI has a band-gap which matches that of TiO_2. Therefore, PANI enhances the electron transfer process but when the PANI film becomes very compact and thick, the electron transfer process might become difficult and the conversion efficiency decreases. Better conversion efficiency (0.26%) obtained when slightly thick film formed (around 25-30 repeated cycles).

Table 1. I-V characteristics of PANI (prepared by CV with different number of cycles)/TiO_2 (prepared by anodization at 20 V in: 0.15 mol L^{-1} HF + 0.5 mol L^{-1} H_3PO_4 for 40 minutes and then annealed at 105℃ for 12 hours and calcinated at 450 ℃ for 2 hours) tested in CoPC dye electrolyte under illumination of 100 mW cm^{-2}.

Number of cycles	I_{sc}/ A	V_{oc}/ V	FF	% η
13	4.47×10^{-4}	0.22	0.95	0.09
18	6.15×10^{-4}	0.18	0.96	0.11
20	8.24×10^{-4}	0.27	0.63	0.14
30	9.40×10^{-4}	0.26	1.0	0.26
40	7.39×10^{-4}	0.25	0.99	0.18

3.2.3. *Effect of illumination*

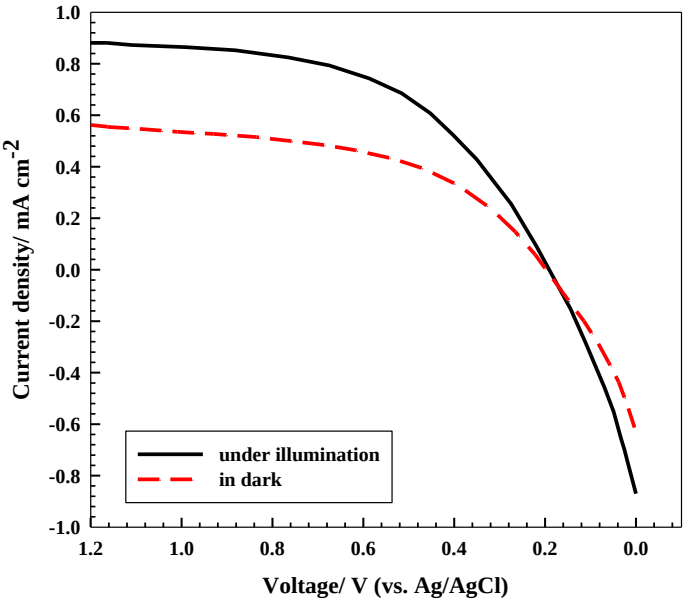

Figure 9. I-V curves of PANI (prepared by 25 repeated CV_s)/TiO_2 tested in CoPC dye electrolyte in dark and under illumination.

The effect of illumination on the enhancement of the conversion efficiency of PANI/TiO_2 NT_s solar cell appears clearly in Figure 9 where PANI/TiO_2 electrode was prepared under the optimized conditions and then tested in 10^{-3} mol L^{-1} CoPC dye in dark and under illumination of 100 mW cm^{-2}. From the results, we noticed that the photoelectrochemical response of the electrode tested under illumination is higher than that tested in dark which illustrates that the cell performance is better under illumination conditions. This might be attributed to excitation of more electrons from the ground state to the excited state in the dye which leads to the enhancement of charge separation and electron transfer processes under illumination.

3.2.4. Effect of dye type

Phthalocyanine (PC) dyes are a promising class of dyes for their interesting photophysical properties, which are dependent on the type and dimension of the metal ion incorporated at the center of the 18π-electron aromatic macroring and on the peripheral groups bound to the molecular skeleton. The large potential of these compounds has been highlighted by several technological applications [29]. In order to extend the photo-response of inorganic semiconductors to the visible region and, thus, to improve the overall energy conversion process, PC dye sensitizers appear promising owing to their large adsorption coefficient in the red and to their thermal and photochemical stability [30]. PC dyes have energy levels matching that of TiO_2. These properties of phthalocyanines make them attractive in the recent research concerning DSSCs. I-V performance parameters of PANI/TiO_2 modified electrode tested in different phthalocyanine dyes under illumination of 100 mW cm^{-2} and PANI films formed with 25 cycles are shown in table 2. CoPC dye sensitized PANI/TiO_2 solar cell showed better conversion compared to CuPC or NiPC dye sensitized PANI/TiO_2 solar cells under 100 mW cm^{-2} illuminations.

Table 2. I-V characteristics of PANI (prepared by 25 repeated cycles)/TiO_2 (prepared by anodization at 20 V in: 0.15 mol L^{-1} HF + 0.5 mol L^{-1} H_3PO_4 for 40 minutes and then annealed at 105 °C for 12 hours and calcinated at 450 °C for 2 hours) tested in different PC dyes solution under illumination of 100 mW cm^{-2}.

Type of dye	I_{sc}/ A	V_{oc}/ V	FF	% η
CoPC	9.66×10^{-4}	0.22	1.0	0.22
CuPC	8.74×10^{-4}	0.24	0.88	0.18
NiPC	6.99×10^{-4}	0.16	0.99	0.11

3.3. Electrochemical impedance spectroscopy (EIS)

EIS is also used for studying the photoelectrochemical properties of PANI/TiO_2 electrodes. The effect of illumination was confirmed by EIS technique. Figure 10 represents the Nyquist plots for PANI/TiO_2 electrode obtained in the dark and under illumination in the presence of 10^{-3} mol L^{-1} CoPC dye solution.

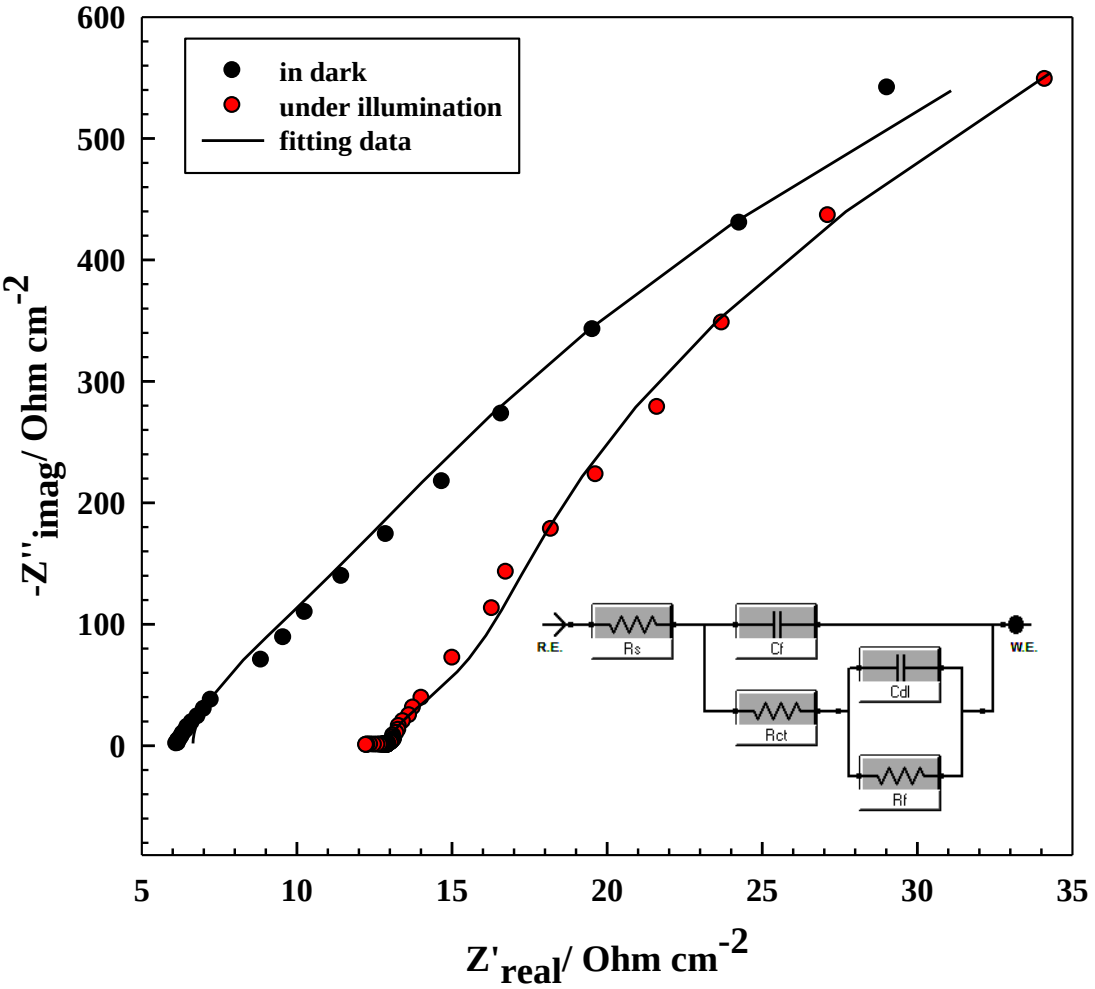

Figure 10. Nyquist plots obtained at open circuit potential for PANI/TiO_2 electrode tested in CoPC dye solution in dark and under illumination. The inset is the equivalent circuit applied for fitting of experimental data.

Table 3 lists the best fitting values calculated from the equivalent circuit shown in Figure 10 (the inset). The model fitted the experimental data well is shown in Figure 10 (points represent experimental data and lines represent fitted data) and provided a reliable description for the electrochemical system. From the circuit, R_s represents the electrolyte resistance, R_f and C_f represent the resistance and capacitance of PANI/TiO_2 film, R_{ct} and C_{dl} represent the charge transfer resistance and double layer capacitance, respectively.

Table 3. The electrochemical parameters, corresponding to Figure 10, estimated from the fitting of experimental data to the equivalent circuit shown as the inset of Figure 10.

PANI/ TiO_2 electrode	R_s / Ω cm^{-2}	C_f / F cm^{-2}	R_{ct}/ Ω cm^{-2}	C_{dl} / F cm^{-2}	R_f/ Ω cm^{-2}
In dark	6.65	2.65×10^{-3}	2.54×10^{3}	1.75×10^{-4}	1.29×10^{4}
Under illumination	12.91	2.53×10^{-3}	8.53×10^{2}	1.88×10^{-4}	1.64×10^{4}

As shown in the Nyquist plots, two resistance-capacitance semicircles were observed. The semicircle at high frequencies was characteristic of the charge transfer process and the diameter of the semicircle equals to the charge transfer resistance (R_{ct}) through PANI/TiO_2 composite. The semicircles shrank remarkably, the diameter of the semicircle was decreased and R_{ct} was decreased under illumination compared with those in dark implying that illumination increased the capacitance and decreased the resistance to Faraday current. This is attributed to the different distribution and density of the electrons under illumination and non-illumination [31]. Thus, the photogenerated electrons excited by illumination enhance the conductivity and consequently improve the photoelectrochemical response and conversion efficiency. This result agrees with the data obtained from I-V curves. It is interesting that two semicircles were seen for PANI/TiO_2 under the conditions of illumination and non-illuminaiton, implying that the reaction at the interface was controlled by two time constants [31]. The natural passive film on the titanium surface was semi-conductive. Thus, the semicircle in the lower frequency could be related to the inner dense passive layer, and the semicircle in the higher frequency range reflected outer less dense TiO_2 layer.

4. CONCLUSIONS

PANI/TiO_2 nanocomposite electrode was prepared via two electrochemical steps: fabrication of TiO_2 NT_s array electrode by constant potential anodization method in HF-H_3PO_4 solution; followed by formation of PANI nanoparticles inside/over TiO_2 NT_s by electropolymerization method. Characterization of PANI/TiO_2 electrode was also reported. XRD analysis showed that anatase phase of TiO_2 prevailed and PANI-modified TiO_2 composite electrode did not change the crystalline structure of neat TiO_2. IR spectroscopy ascertained the formation of PANI film. The applicability of PANI/TiO_2 nanocomposite electrode to $DSSC_s$ using different metal phthalocyanine dyes was studied in dark and under illumination. CoPC dye sensitized solar cell based on PANI/TiO_2 composite electrode showed better photoelectrochemical conversion efficiency (0.26%) compared to neat TiO_2 electrode (0.18%) under illumination of 100 mW cm^{-2} with good stability. CoPC dye sensitized PANI/TiO_2 solar cell showed better conversion efficiency under illumination compared to dark conditions (0.11%).

ACKNOWLEDGMENT
The authors would like to acknowledge the financial support from Cairo University through the Vice President Office for Research Funds.

References

1. B.O' Reagan, M. Grätzel, *Nature* 353 (1991) 737.
2. J. Nowotny, T. Bak, M.K. Nowotny, L.R. Sheppard, *Int. J. Hydrogen Energy* 32 (2007) 2609.
3. X. Feng, K. Shankar, O.K. Varghese, M. Paulose, T.J. Latempa, C.A. Grimes, *Nano Lett*. 8 (2008) 3781.

4. G.K. Mor, K. Shankar, M. Paulose, O.K. Varghese, C.A. Grimes, *Nano Lett*. 6 (2005) 215.
5. M. Paulose, K. Shankar, O.K. Varghese, G.K. Mor, B. Hardin, C.A. Grimes, *Nanotechnology* 17 (2006) 1446.
6. A.Hagfeldt, M. Grätzel, *Acc. Chem. Res*. 33 (2000) 269.
7. M. Grätzel, *J. Photochem. Photobiol. A Chem*. 164 (2004) 3.
8. M. Junghanel, H. Tributsch, *J. Phys. Chem*. B 109 (2005) 22876.
9. A.L. Thomas, Ed. ‘‘Phthalocyanine Research and Applications, CRC Press, Boston, 1990.
10. C.C. Wamser, H. -Sung Kim, J. -Kook Lee, *Opt. Mater*. 21 (2002) 221.
11. C.K. Chiang, C.R. Fincher, Y.W. Park, A.J. Heeger, H. Shirakawa, E.J. Louis, S.C. Grau, A.G. MacDiarmid, *Phys. Rev. Lett*. 39 (1977) 1098.
12. W.S. Huang, B.D. Humphrey, A.G. MacDiarmid, *J. Chem. Soc. Faraday Trans*. 82 (1986) 2385.
13. J.C. Fatuch, M.A. Soto-Oviedo, C.O. Avellaneda, M.F. Franco, W. Romão, M. De Paoli, A.F. Nogueira, *Synth. Met*., 159 (2009) 2348.
14. M.R. Karim, J.H. Yeum, M.S. Lee, K.T. Lim, *React. Funct. Polym*. 68 (2008) 1371.
15. Z. Zhang, Y. Yuan, L. Liang, Y. Cheng, H. Xu, G. Shi, L. Jin, *Thin Solid Films* 516 (2008) 8663.
16. K. Murakoshi, R. Kogure, Y. Wada, S. Yanagida, *Sol. Energy Mater. Sol. Cells* 55 (1998) 113.
17. L. Giribabu, C.V. Kumar, V.G. Reddy, P.Y. Reddy, C.S. Rao, S. -Rim Jan, J. -Ho Yum, M.K. Nazeeruddin, M. Grätzel, *Sol. Energy Mater. Sol. Cells* 91 (2007) 1611.
18. N. F. Atta, H. M.A. Amin, M. W. Khalil, A. Galal, *Int. J. Electrochem. Sci*. 6 (2011) 3316.
19. D. E. Stilwell, S.M. Park, *J. Electrochem. Soc*. 135 (1988) 2254.
20. C.H. Yang, T.C. Wen, *J. Appl. Electrochem*. 24 (1994) 166.
21. Y. Wei, Y. Sun, X. Tang, *J. Phys. Chem*. 93 (1989) 4878.
22. S.K. Mohapatra, M. Misra, V.K. Mahajan, K.S. Raja. *J. Catal*. 246 (2007) 362.
23. W. Wang, O.K. Varghese, M. Paulose, C.A. Grimes, *J. Mat. Res*., 19 (2004) 417.
24. X. Li, D. Wang, G. Cheng, Q. Luo, J. An, Y. Wang, *Appl. Catal. B: Environ*. 81 (2008) 267.
25. M. R. Karim, J. H. Yeum, M. S. Lee, K. T. Lim, *React. Funct. Polym*. 68 (2008) 1371.
26. X. Sui, Y. Chu, S. Xing, C. Liu, *Mater. Lett*. 58 (2004) 1255.
27. M.R. Karim, K.T. Lim, M.S. Lee, K. Kim, J.H. Yeum, *Synth. Metals* 159 (2009) 209.
28. N.R. de Tacconi, C.R. Chenthamarakshan, G. Yogeeswaran, A. Watcharenwong, R.S. de Zoysa, N.A. Basit, K. Rajeshwar, *J. Phys. Chem*. B 110 (2006) 25347.
29. D. Wróbel, A. Boguta, *J. Photochem. Photobiol. A: Chem*. 150 (2002) 67.
30. C. Ingrosso, A. Petrella, M.L. Curri, M. Striccoli, P. Cosma, P.D. Cozzoli, *Appl. Surf. Sci*. 246 (2005) 367.
31. Z. Li, Z. Pengyi, C. Songzhe, *Chin. J. Catal*. 28(2007) 299.